JEBAT, 2024, Vol 7, No 2, 49-57
https://doi.org/10.54987/jebat.v7i2.1037

HIBISCUS PUBLISHER

JOURNAL OF ENVIRONMENTAL BIOREMEDIATION AND TOXICOLOGY

Website: http://journal.hibiscuspublisher.com/index.php/JEBAT/index

Enhancing Pharmaceutical Wastewater Treatment Through Adsorption With Rice Husk –derived Cellulose Nano Crystals as an Innovative Adsorbent

Abubakar M. Hammari[1,2]*, U. D. Hamza[1], Maryam Ibrahim[1], Kabir Garba[1] and I.M. Muhammad[1]

[1]Department of Chemical Engineering, Faculty of Engineering, Abubakar Tafawa Balewa University, P.M.B. 0248, Bauchi, Nigeria.
[2]Department of Biochemistry, Faculty of Science, Gombe State University, P.M.B. 127, Tudun Wada, Gombe, Nigeria.

*Corresponding author:
Abubakar M. Hammari,
Department of Chemical Engineering,
Faculty of Engineering,
Abubakar Tafawa Balewa University,
P.M.B. 0248,
Bauchi,
Nigeria.
Email: abhammari@gsu.edu.ng; abhammari15@gmail.com

HISTORY

Received: 28th Aug 2024
Received in revised form: 12th Nov 2024
Accepted: 20th Dec 2024

KEYWORDS

Cellulose nanocrystals (CNCs)
Agricultural waste
Rice-husk
Adsorption efficiency
Metronidazole removal

ABSTRACT

This study investigates the adsorption of the antibiotic metronidazole using cellulose nanocrystals (CNC) extracted from rice husk. The research highlights the importance of removing antibiotic contamination from water bodies and explores the potential of CNC as an adsorbent. The synthesis of CNC from rice husk achieved a yield of 26.46% through a series of pretreatment processes, including bleaching and acid hydrolysis. The CNC adsorbent was characterized using FTIR, BET, SEM, and XRD to determine its structural and surface properties, revealing a total pore volume of 0.225 cm^3 and a micropore volume of 0.233 cm^3. The effects of various parameters, including pH (with maximum adsorption at pH 9), temperature (optimal at 50°C), and time (maximum adsorption at 60 min), were also considered. The adsorption rate of metronidazole by CNC-RH increased with higher adsorbent dosage and adsorbate concentration. Adsorption kinetics were evaluated, with the pseudo-second-order model found to be the most appropriate. Adsorption isotherms were also studied, with the Freundlich model displaying excellent linearity ($R^2 = 1$). Thermodynamic parameters were calculated, including a negative ΔG (-103.566, -105.976, -110.796, -115.616, -120.46 J/mol), indicating a spontaneous process, a ΔS value of 0.482 J/molK, and a positive ΔH value of 40.07 J/mol, suggesting an endothermic process. Overall, this study offers valuable insights into the adsorption behavior of metronidazole using CNC derived from rice husk and underscores the importance of the selected parameters in the adsorption process.

INTRODUCTION

Although water seems abundant on Earth, its accessible, usable form is limited. Rapid population growth and industrialization have led to a surge in water demand, while the natural water supply remains unchanged [1]. Although water seems abundant on Earth, its accessible, usable form is limited. Rapid population growth and industrialization have led to a surge in water demand, while the natural water supply remains unchanged [2]. Pharmaceuticals encompass a diverse group of compounds with varying structures, functions, and behaviors. Water plays a crucial role in pharmaceutical manufacturing, from raw material handling to drug purification, resulting in substantial pharmaceutical wastewater generation. This wastewater typically contains organic solvents and pharmaceutical intermediates, many of which pose risks to human health. Therefore, efficient treatment of pharmaceutical wastewater is essential for mitigating water pollution [3]. Due to its cost-effectiveness, simplicity, and efficiency, adsorption is widely employed as a method for treating wastewater. Surface functional groups, along with their concentration, are key factors that influence the adsorbent's capacity and the overall pollutant removal process [4]. Among various wastewater treatment techniques, adsorption is particularly advantageous due to its molecular-level selectivity, low energy requirements, and ease of operation [5].

It involves the attachment of dissolved molecules onto an adsorbent surface through physical and chemical interactions. The cost of the adsorbent is a crucial factor, making low-cost materials, such as agricultural and industrial by-products, highly desirable. In recent years, various low-cost adsorbents, including cucumber peels, sawdust, bagasse, durian leaf powder, watermelon seed hulls, grape pulp, chitosan, kenaf core fibers, hazelnut shells, rice husk, and Delonix regia plant leaves, have

been explored for wastewater treatment [6]. Using agricultural waste for pharmaceutical wastewater treatment not only addresses solid waste disposal challenges but also benefits the economy by providing farmers and the agro-industry with an additional revenue source. This has led to increased research interest in developing porous adsorbents from agricultural materials for removing pollutants from pharmaceutical effluents. Agricultural biomass is abundant, cost-effective, and renewable, making it an attractive option for water treatment applications [7]. As the most plentiful biopolymer found in nature, cellulose forms a key structural element in the cell walls of plants [8]. Native cellulose is composed of repeating β-(1→4)-D-glucopyranose units forming nanofibrils, which typically range from 3 to 10 nm in diameter and extend to several microns in length, depending on the plant source. Research on nanocellulose has grown significantly over the past decade and is expected to continue expanding [9].

Nanocellulose can refer to various materials, including nanofibrillated cellulose (NFC), microfibrillated cellulose (MFC), cellulose nanocrystals (CNC), and bacterial cellulose (BC), each differing in dimensions. This study focuses on cellulose nanocrystals (CNC), which are needle-like structures with diameters of 5–10 nm and lengths of 100–200 nm [10]. Nanocellulose is renewable, biodegradable, mechanically strong, and has a high surface area. Its specific properties, such as surface charge and dimensions, vary depending on the preparation method and cellulose source. To enhance its functionality, nanocellulose can be chemically modified to introduce functional groups that facilitate the adsorption of molecules such as peptides, antibodies, metals, and drugs. Functionalized nanocellulose has potential applications in diverse fields, including packaging, pharmaceuticals, wastewater treatment, and cosmetics [11-14].

Pharmaceutical contaminants in water pose significant environmental and health risks, including high toxicity to aquatic life, the proliferation of antibiotic-resistant bacteria, endocrine disruption in humans and animals, and the presence of pharmaceutical residues in aquatic ecosystems. Adsorption has been recognized as an effective approach for pharmaceutical removal from wastewater, as other methods—such as ion exchange, flocculation, and solvent extraction—suffer from limitations such as incomplete removal, high operational costs, energy-intensive processes, and excessive chemical usage [15]. Pharmaceutical pollutants enter water systems during production and can contaminate both surface and groundwater, posing serious environmental threats. Meanwhile, agricultural waste is often discarded, contributing to environmental pollution [16].

To the best of the researcher's knowledge, the use of rice husk as an adsorbent for pharmaceutical effluents has not been widely reported. Utilizing agricultural waste as an adsorbent could help mitigate environmental risks while also generating economic benefits for farmers. The presence of pharmaceutical contaminants in wastewater can have adverse health effects, including respiratory distress upon inhalation and gastrointestinal symptoms, nausea, vomiting, sweating, diarrhea, and methemoglobinemia upon ingestion [17]. Acute exposure may also lead to conditions such as cyanosis, Heinz body formation, jaundice, quadriplegia, and tissue necrosis in humans. Therefore, further research is needed to explore the use of agricultural waste for water purification through adsorption. Investigating the equilibrium, kinetics, and thermodynamics of rice husk-based adsorption will help determine its pharmaceutical removal efficiency and establish optimal design parameters for the adsorption process. The aim of this research is to conduct equilibrium isotherms, kinetics and thermodynamic studies of pharmaceutical adsorption on rice husk derived Cellulose nano-crystal as an innovative adsorbent,

MATERIALS AND METHODS

Sample collection

Agro-waste (Rice Husk) was collected from a rice mill at Anguwa Uku in the Gombe Local Government Area of Gombe State, Nigeria.

Extraction of α-Cellulose

A 500 g sample of rice husk was weighed using an electronic balance and placed in a stainless steel container. A 2% (w/v) sodium hydroxide solution was prepared and added to the sample, ensuring thorough mixing to wet the material. The mixture was then heated in a water bath at 80°C for 4 hs to facilitate delignification. After this process, the mixture was filtered using a cloth sieve, washed extensively with water, and re-filtered. The delignified material was subsequently treated with a 1:1 dilution of sodium hypochlorite solution (3.0 L) at 95°C for 30 min in a water bath for bleaching. Following this, the material was filtered and washed thoroughly using a sieve cloth with ample water. It was then placed back into the stainless steel container, and 2.0 L of a 17.5% (w/v) sodium hydroxide solution was added while stirring. This mixture was heated in a water bath at 80°C for 1 h to extract α-cellulose.

The obtained material was washed with water, filtered, and subjected to a second bleaching step using a 1:1 dilution of sodium hypochlorite (1 L) in a water bath at 80°C for up to 15 min. The sample was then filtered again using a sieve cloth and rinsed thoroughly with water five times until it tested neutral with litmus paper. The washed material was pressed into a large lump, broken into smaller pieces, and dried in a hot air oven at 60°C for 60 min. The final product was labeled as rice husk α-cellulose and stored for further processing.

Preparation of Cellulose Nanocrystals (Acid Hydrolysis Method)

The procedure for producing cellulose nanocrystals (CNCs) was adapted from Ohwoavworhua et al. [19] with slight modifications. The extracted α-cellulose was weighed and subjected to hydrolysis using 1.6 L of hydrochloric acid at boiling temperature for 40 min in a water bath. After hydrolysis, the hot acid mixture was poured into excess tap water in a bucket and stirred vigorously. The suspension was allowed to settle for 18 hs, after which the sedimented material was collected by filtration using a sieve cloth. The residue was extensively washed with water until it tested neutral with litmus paper. The washed material was then broken into small lumps and dried in a hot air oven at 60°C for 60 min. The final yield was determined to be 378 g and was labeled as rice husk cellulose nanocrystals.
To refine the nanocrystals, they were ground using a porcelain mortar and pestle, and the fractions were sieved through a No. 60 mesh. The percentage yield was calculated, and the prepared crystalline cellulose was analyzed for its adsorbent properties.

Percentage Yield of RH-CNCs

Percent yield was calculated using the following formula;-

$$\% \text{ Yield} = W / W_o \times 100 \quad \text{(Eqn. 1)}$$

Where
W_o = Initial weight of the raw material.
W = Weight of dried hydrolysed cellulose.

Adsorbent characterization
The characterization of CNC adsorbent was carried out to determine the pH of the adsorbent, density and water binding capacity (WBC). Other techniques includedFourier transform infra-red spectroscopy (FTIR), scanning electron microscope (SEM), X-ray diffraction (XRD), and Brunauer Emmett-Teller (BET).

Fourier Transform Infrared (FTIR) Spectroscopy
FTIR spectroscopy was employed to detect and identify the functional groups present on the surface of the adsorbent. The FTIR spectra of the adsorbent were recorded prior to the adsorption process using a spectrophotometer. A 0.1 g sample of each adsorbent was blended with 1 g of spectroscopy-grade KBr and compressed using a hydraulic press (15 KPa/cm^2) to form translucent pellets. To eliminate any interference from moisture or CO_2, the disks were heated in an oven at 105°C for 4 hs. The FTIR spectra were recorded within the wavenumber range of 4000–450 cm^{-1}.

Scanning Electron Microscopy (SEM)
Structural changes in the samples were examined using a Phenom ProX SEM (PhenomWorld, Eindhoven, The Netherlands). The sample was taken, placed on double adhesive which was on a sample stub, and sputter coated (using coater by quorum technologies model Q150R), with 5nm of gold. The coated sample was then placed in the SEM chamber and initially viewed using NaVCaM mode for focusing and fine adjustments. Afterward, the sample was transferred to SEM mode, where automatic brightness and contrast adjustments were applied. The surface morphologies at different magnifications were captured and stored for analysis.

X-ray Diffraction (XRD) Analysis
An X-ray diffractometer was used to assess the crystalline structure and diffraction patterns of the cellulose sample. Cu-Kα radiation at 40 kV and 25 Ma was used to record the diffractograms. The powdered sample was compressed into 2.50 cm diameter pellets under a pressure of 50 MPa. The XRD pattern was recorded in continuous mode over a 2θ range of 5° to 70° at a scan rate of 120 min^{-1}.

Brunauer-Emmett-Teller (BET) Analysis
BET analysis was carried out to determine the surface area, pore volume, and pore size distribution of the CNC sample. Nitrogen adsorption isotherms were obtained using a Micromeritics ASAP 2010 analyzer. Prior to measurement, 0.05 g of CNC sample was conditioned by outgassing in a vacuum at 250°C overnight to eliminate moisture and other adsorbed gases. The sample was then weighed to ensure accuracy before being placed in glass tubes and exposed to nitrogen gas at 77K under incremental pressure conditions. The quantity of adsorbed gas molecules was automatically recorded and retrieved via the instrument's computing system.

Adsorption Experiment
Preparation of Standard Solutions
Analytical-grade metronidazole was obtained from the Pharmaceutics Laboratory, Gombe State University. A stock solution (1000 mg/L) was prepared by dissolving 1 g of powdered metronidazole in 1 L of distilled water. Experimental solutions of desired concentrations were prepared by diluting the stock solution.

Adsorption Experiment Design
Table 1 summarizes the experimental design for the adsorption test. The effect of adsorbent dose on the adsorption of metronidazole (MNZ) was investigated by adding varying amounts of CNC-RH (0.5, 1.5, 2.0, 2.5, and 3.0 g) into 100 mL of MNZ solution (50 mg/L) at normal pH and room temperature. The samples were continuously agitated at 200 rpm for 60 min, after which the adsorbent was separated using Whatman filter paper. The final concentration of MNZ in the solution was determined using a UV-Vis spectrophotometer (Shimadzu, Double Beam, UV-1800, Japan) in spectrophotometric mode.
To study the effect of temperature and initial MNZ concentration, batch adsorption experiments were conducted using a 250 mL airtight Erlenmeyer flask containing 100 mL of MNZ solution at varying concentrations. The optimum adsorbent dosage (2.0 g) was selected based on previous experiments [29]. The mixture was continuously agitated on an orbital shaker at a constant speed of 200 rpm. The effect of initial MNZ concentration (50, 100, 150, 200, and 250 mg/L) and temperature (298, 303, 313, 323, and 333 K) was evaluated. At predetermined time intervals (60 min), the flasks were removed from the shaker, and the samples were filtered. The final MNZ concentration in the supernatant solution was analyzed using a UV-Vis spectrophotometer. All the above methodologies are according to [18-21]

Adsorption Capacity and Removal Efficiency
The equilibrium adsorption capacity (q_e) of MNZ was calculated using the following equation:

$$q_e = \frac{(C_o - C_e)V}{M} \quad \text{(Eqn. 2)}$$

$$PercentageMNZRemoval = \frac{(C_o - C_e)V}{M} X\ 100 \quad \text{(Eqn. 3)}$$

Where:
q_e = amount of MNZ adsorbed at equilibrium (mg/g)
C_o = initial MNZ concentration (mg/L)
C_e = MNZ concentration at equilibrium (mg/L)
M = mass of the adsorbent (g)
V = volume of the solution (L)

This methodology ensured accurate determination of MNZ removal efficiency and adsorption performance under different experimental conditions.

Table 1. Experimental design for batch adsorption technique.

Parameters	Initial Conc. ppm	Dosage (g)	pH	Time (min)	Temperature (K)
Temperature	50	2.0	6.5	60	298, 303,313,323,343
Dosage	50	0.5,1.5,2,2.5,3	6.5	60	298
Initial Conc.	50,100,150,200,250	2.0	6.5	60	298
pH	50	2.0	3,5,7,9,10	60	298
Time	50	2.0	6.5	30,60,90,120,150	298

Langmuir isotherm

The Langmuir equilibrium model revolves around the concept of a monolayer with an extreme adsorption ability for the adsorbent. This implies that each active binding site can host only one molecule, assuming consistent adsorption energy across all such sites. Furthermore, the model postulates that the adsorbed molecules remain stationary on the surface and do not undergo movement or interaction with neighboring molecules, as explained by [22] The Langmuir equation, often expressed in a linear form, captures these principles.

$$\frac{C_e}{q_e} = \frac{1}{q_m k_l} + \frac{C_e}{q_m} \quad \text{(Eqn. 4)}$$

The Langmuir isotherm model quantifies the adsorption process by considering the equilibrium amount of dye adsorbed (qe) in relation to the maximum adsorption capacity (qm) when saturation is reached. Ce denotes the isotherm concentration, and kl represents the Langmuir constant, which is associated with the strength of adsorbate binding to the adsorbent surface.

Freundlich isotherm

Moving to the Freundlich isotherm, this is an experimental equation which proves highly effective in relating the partitioning of solutes between solid and aqueous stages at overload. It operates under the statement of an exponential difference in site energies on the adsorbent as a logarithmic decline in temperature of adsorption, as outlined by [23].

The linearized form of the Freundlich equation can be expressed as:

$$Log q_e = Log K_f + \frac{1}{n} Log C_e \quad \text{(Eqn. 5)}$$

In this equation, K_F represents the Freundlich constant, a measure of adsorption capacity, while n signifies the intensity of adsorption. The value of n holds particular significance:

-n = 1 agrees to linear adsorption
-n < 1 implies a chemical practice
-n > 1 indicates a physical practice [24].

Adsorption kinetics experiments

The prediction of adsorption kinetics is imperative for the effective design of adsorption systems. Kinetic parameters, which offer insight into adsorption rates, are crucial for process modeling and design. The successful utilization of adsorption methods necessitates the development of cost-effective, readily accessible, and plentiful adsorbents characterized by well-known kinetic model values and sorption traits, as emphasized by [22]. The analysis of adsorption kinetics provides a forecast of how adsorption advances over time until equilibrium is achieved. Furthermore, understanding the adsorption tool holds significance for plan considerations. Therefore to unravel the adsorption mechanism of pharmaceuticals, pseudo-first-order and pseudo-second-order kinetics models have remained employed, as explored by [22].

Pseudo-first-order kinetic model

Beginning with the pseudo-first-order kinetic model, Lagergren's kinetics balance, which was among the first to describe liquid-solid system adsorption based on solid capacity, has been termed pseudo-first order due to its reliance on adsorption capacity rather than solution concentration. The linear representation of this model is:

$$\mathrm{Ln}(q_e - q_t) = ln q_e - k_1 t \quad \text{(Eqn. 6)}$$

Here, q_e and q_t represents the total amount of pollutant adsorbed per unit mass of the adsorbent at equilibrium and at various time intervals (t), respectively. The model's adsorption rate constant is denoted as k_1 (min-1). By plotting $\ln(q_e - q_t)$ against time t, k_1 and calculated q_e can be obtained from the slope and intercept, respectively [22].

Pseudo-Second-Order kinetic model

The pseudo-second-order kinetic model is expressed by Enenebeaku et al., [30].

$$\frac{t}{q_t} = \frac{1}{k_2 q_e^{\,2}} + \frac{1}{q_e} \quad \text{(Eqn. 7)}$$

Here, k_2 represents the pseudo-second-order adsorption rate constant (g/mg.min), and qe is the amount of MNZ adsorbed (mg/g) at equilibrium. The initial adsorption rate, h (mg/g·min), is given by:

$$h = k^2 q_e \quad \text{(Eqn. 8)}$$

A linear relationship between t/qt and t enables the computation of k2/h, and calculated qe. The choice of applicable models is typically based on the correlation coefficient (R^2) and the degree of agreement between experimental and calculated qe values, as detailed by [25].

Adsorption thermodynamics experiments

The thermodynamic adsorption experiments were conducted similarly to the temperature effect studies in batch adsorption. However, in this case, the flask containing the adsorbent-drug mixture was agitated in an incubator shaker set at a predetermined temperature. The rate of drug removal by rice husk CNC powder was monitored throughout the process. To evaluate the feasibility and spontaneity of the adsorption process, standard thermodynamic parameters—including enthalpy (ΔH), entropy (ΔS), and free energy (ΔG) were determined by conducting experiments at varying temperatures. These parameters are essential for understanding the heat changes and energetic favorability of the adsorption process. The thermodynamic properties were calculated using the following equations [6].

$$k_e = \frac{qe}{C_e} \quad \text{(Eqn. 9)}$$

$$ln k_e = \frac{\Delta S^\circ}{R} - \frac{\Delta H^\circ}{RT}$$

(Eqn. 10)

$$\Delta G^\circ = \Delta H^\circ - T\,\Delta S^\circ$$

(Eqn. 11)

In this context, K_e denotes the equilibrium constant, q_e indicates the amount of pollutant adsorbed (mg/dm³), C_e refers to the equilibrium concentration in mg/L, *R* is the universal gas constant (8.314 J/mol·K), and *T* is the absolute temperature in Kelvin. The thermodynamic parameters, standard enthalpy (ΔH) and standard entropy (ΔS), are determined from the slope and intercept of the plot of ln(Ke) versus 1/T.

These are some of the commonly used adsorption models. Researchers choose the appropriate model based on the type of adsorption (e.g.physisorption or chemisorption) and the specific characteristics of the adsorption system being studied. Fitting experimental data to these models helps in understanding the adsorption behavior and obtaining important parameters like adsorption capacity, surface area, and affinity of the adsorbate-adsorbent system.

RESULTS AND DISCUSSIONS

Percentage yield

Rice husk yields significantly less CNC. This lower yield can be attributed to the composition of rice husk, which contains a substantial amount of silica (about 15-20%), lignin, and hemi cellulose. These non-cellulosic components need to be removed through pre-treatment processes, which can reduce the overall efficiency of cellulose extraction and conversion to CNC. The lower yield suggests additional processing steps and treatments are necessary to enhance CNC production from rice husk [26].

Characterization Results

The characterization results of the study are presented in the section below:

FTIR characterization of CNC –RH

The FTIR spectrum of CNC-RH which gave insight into the nature of their surface functional groups and structures over frequency range of 4000 to 500cm is presented in **Fig. 1.**

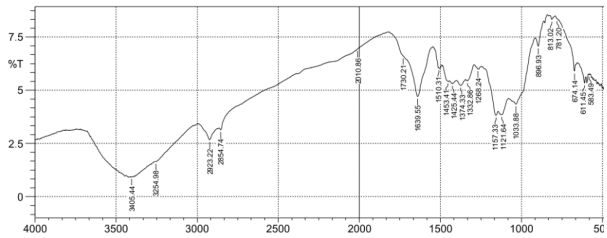

Fig. 1. FTIR spectra of cellullose nano crystals derived from rice husk.

The FTIR analysis revealed more than five peaks, suggesting that the analyzed compound is complex. The presence of absorption bands in the single-bond region (2500–4000 cm^{-1}) includes a broad band at 3250–3650 cm^{-1}, indicating hydrogen bonding, with hydroxyl group peaks specifically observed at 3254.98 cm^{-1} and 3405.44 cm^{-1}. The absence of a sharp peak around 350 cm^{-1} suggests no oxygen-related bonding.

A characteristic aldehyde peak appears between 2700–2800 cm^{-1}, while a double-bond region is identified between 1500–2000 cm^{-1}. Additionally, a strong absorption band is detected at 3405.44 cm^{-1}. The presence of a double olefinic bond is confirmed at 896.93 cm^{-1}. Aromatic compounds are indicated by a strong absorption for ortho-substituted at 781.20 cm^{-1} and para-substituted at 813.02 cm^{-1}. Based on these findings, the material contains hydrated components and double bonds, lacks oxygen-related bonding and triple bonds, and has 22 peaks, confirming it as a large organic compound.

SEM characterization

Scanning Electron Microscopy (SEM) is an essential technique for analyzing the morphology and fundamental physical properties of an adsorbent's surface. It provides valuable insights into particle size, shape, and porosity. In this study, SEM micrographs were used to examine the surface morphology of CNC-RH samples (A), (B), and (C) at magnifications of 500×, 1000×, and 2000× respectively.

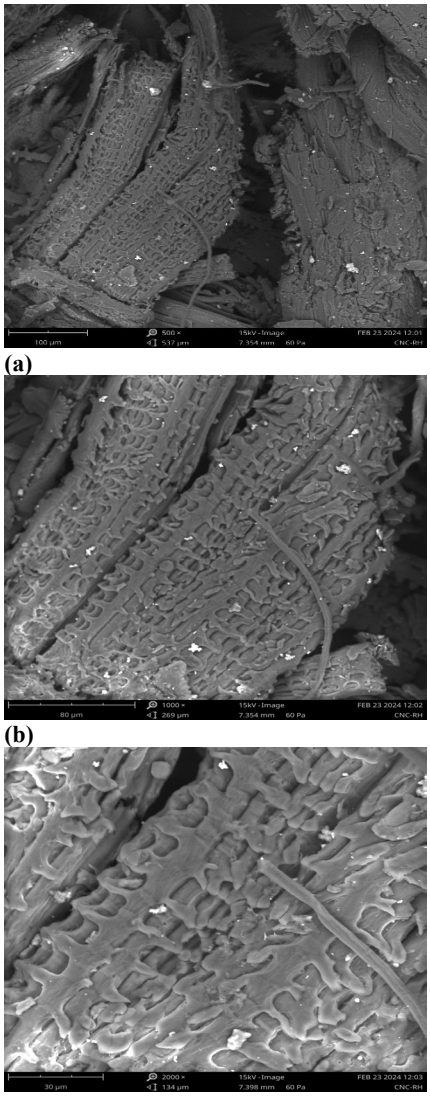

Fig. 2. SEM micrograph of cellullose nano crystals derived from rice husk at different magnifications of 500, 100 and 200 µg denoted by a, b, and c, respectively.

BET characterization of CNC-RH

The BET characterization provides insights into the surface textural properties of CNC-RH. It includes key parameters such as the multi-point BET surface area, BJH total pore volume, BJH average pore width, and HK micropore volume. The results of these analyses are presented below.

Table 2. Surface textural properties of cellullose nano crystals derived from rice husk material.

BET Surface Area (m^2/g)	Total Pore Volume (cm^3/g)	Micro Pore Volume (cm^3/g)	Average Pore With (nm)
459.604	0.225	0.233	3.866

The CNC-RH displays very large surface are moderate total pore volume (**Table 2**). This result shows that the modification of rice husk results in higher surface area and total pore volume [27,28].

XRD Characterization

Fig. 3 presents the XRD patterns of CNC-RH, revealing a series of characteristic peaks at 2θ = 14°, 3°.48°, 3°, 14°, 9°, 5°, 13°, 14°, and 4°, corresponding to their respective indices of 19.900, 4.458, 478, 7.58, 4109, 8.6, 0.682, and 0.459. These peaks align with the results reported in previous research by [29], confirming the structural consistency of CNC-RH.

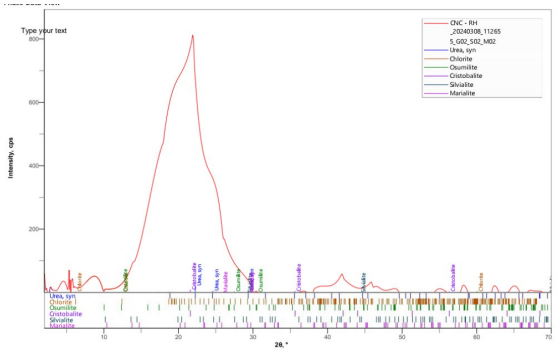

Fig. 3. XRD characterization for cellullose nano crystals derived from rice husk.

Batch adsorption study

Effect of Initial Concentration on Adsorption

The adsorption of MNZ onto CNC-RH was influenced by the initial adsorbate concentration, with maximum adsorption observed as the concentration increased from 50 mg/L to 250 mg/L. The percentage removal of MNZ at initial concentrations of 50 mg/L, 100 mg/L, 150 mg/L, 200 mg/L, and 250 mg/L was 81.084%, 91.516%, 92.66%, 94.500%, and 96.107%, respectively. This trend can be attributed to the mass transfer phenomenon between the adsorbent and adsorbate. At lower concentrations (e.g., 50 mg/L), the available adsorption sites on the CNC-RH surface are quickly occupied by sorbate molecules, leading to a lower adsorption capacity of 1.458 mg/g. However, at higher initial concentrations (e.g., 200 mg/L), the increased number of adsorbate molecules facilitates a more effective adsorbent-adsorbate interaction, resulting in a higher adsorption capacity of 3.0 mg/g. Therefore, an increase in initial concentration enhances the overall adsorption process of [30].

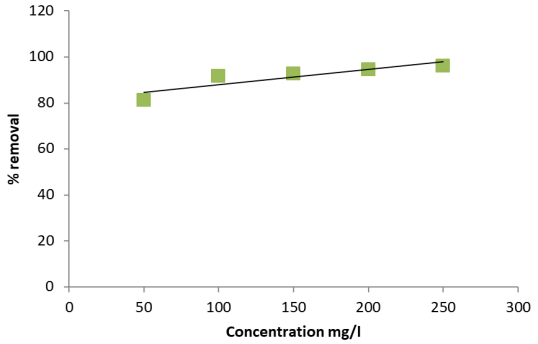

Fig. 4. Effect of the initial concentration for the adsorption of metronidazole antibiotic using CNC-RH.

Effect of Adsorbent Dose on MNZ Adsorption

To assess the effect of adsorbent dosage on MNZ removal, varying amounts of CNC-RH (0.5 to 3.0 g) were added to 100 mL of a 50 mg/L MNZ solution under ambient conditions and neutral pH. **Fig. 6** illustrates the percentage removal of MNZ by CNC-RH at varying adsorbent dosages. The results indicate that adsorption efficiency increased with higher adsorbent doses, with CNC-RH effectively removing a significant amount of MNZ even at the lowest dose of 0.5 g. However, beyond a dosage of 1.5 g, no significant increase in antibiotic removal was observed, suggesting that 1.5 g is the optimal adsorbent dose and was used in subsequent experiments. The high adsorption capacity of CNC-RH at lower dosages can be attributed to its large surface area and pore volume. The initial increase in MNZ removal with higher adsorbent doses was due to the availability of more adsorption sites and surface area. Nevertheless, as the adsorbent dosage increased further, some adsorption sites became saturated, leading to a decrease in adsorption capacity despite the overall increase in removal efficiency.

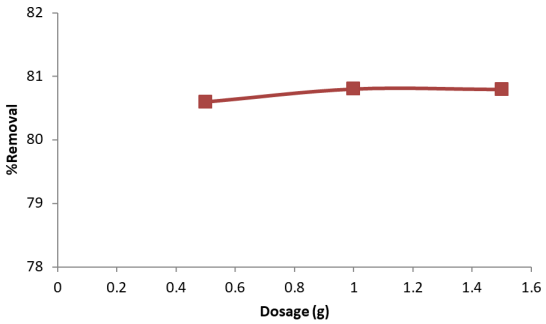

Fig. 5. Effect of adsorbent dosage for the adsorption of metronidazole antibiotic using CNC-RH.

Effect of Contact Time on MNZ Adsorption

The adsorption of MNZ varies with changes in the initial concentration of CNC-RH and contact time. The effect of contact time (30, 60, 90, 120, and 150 min) on MNZ adsorption is presented in **Fig. 6**. The results indicate that the adsorption process is rapid, with the majority of MNZ being adsorbed within the first 60 min. Equilibrium was reached at 120 min, beyond which no significant further adsorption occurred.

The rapid initial adsorption can be attributed to the abundance of available adsorption sites at the beginning of the process, allowing MNZ molecules to bind efficiently. As these sites became saturated, the adsorption rate declined, leading to equilibrium. Although equilibrium was reached within 120 min, the experiment was extended to 150 min to ensure complete stabilization. The equilibrium time is specific to each adsorbent and varies depending on its surface area and porosity. Previous studies have reported equilibrium times ranging from 90 to 150 min, reinforcing the observed trend in this study.

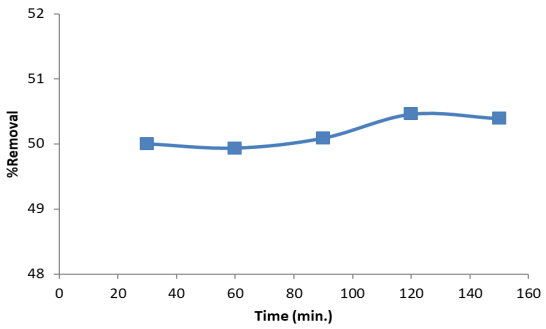

Fig. 6. The effect of contact time for the adsorption of metronidazole antibiotic using CNC-RH.

Effect of Solution pH on MNZ Adsorption

Solution pH plays a crucial role in the adsorption process by influencing the aqueous chemistry and the binding sites on the

adsorbent surface. **Fig. 7** illustrates the effect of pH on the percentage removal of MNZ by CNC-RH. The initial pH of the solution was adjusted between 3 and 11 to determine the optimal pH for maximum adsorption. The results indicate that MNZ adsorption increased as the pH was raised, reaching a maximum adsorption efficiency of 81.846% at pH 9, compared to 80.786% at lower pH levels. However, beyond pH 9, the adsorption efficiency declined as the pH increased to 11. This suggests that pH 9 is the optimal condition for MNZ adsorption onto CNC-RH.

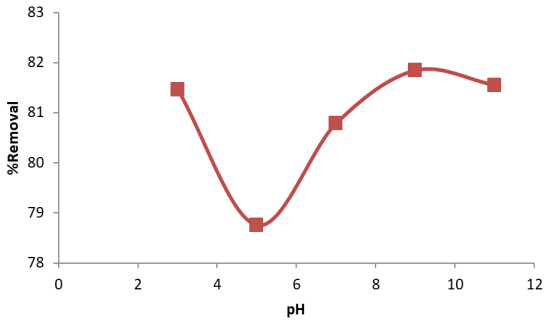

Fig. 7. The effect pH for the adsorption of metronidazole antibiotic using CNC-RH.

Effect of Temperature on MNZ Adsorption

The adsorption results indicate that as the temperature increased from 25 °C to 60 °C, the percentage removal of MNZ by CNC-RH initially rose from 50% to a maximum of 56.793% at 50 °C. This initial increase in adsorption capacity can be attributed to the enhanced mobility of adsorbate molecules due to reduced viscosity, allowing better interaction with the adsorbent's external surface and internal pores. However, when the temperature exceeded 50°C, a decline in adsorption capacity was observed. This decrease is likely due to the weakening of adsorptive forces between the adsorbate and adsorbent at higher temperatures, reducing the overall adsorption efficiency. In general, the adsorption of organic and chemical compounds is typically an exothermic process, meaning higher temperatures can negatively impact adsorption performance.

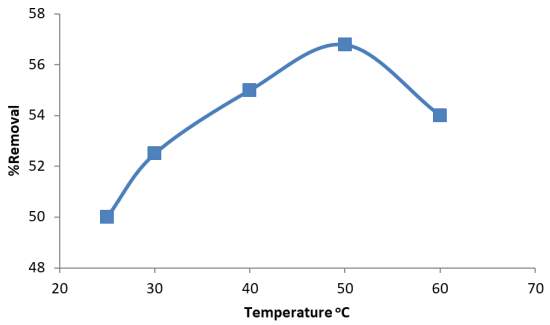

Fig. 8. The effect of temperature for the adsorption of metronidazole antibiotic using CNC-RH.

Adsorption Isotherm Models for Metronidazole Antibiotic Using CNC-RH

Adsorption isotherm studies describe the interaction between the adsorbate and the adsorbent, providing insight into the theoretical maximum adsorption capacity of an adsorbent for a given adsorbate [26]. To characterize the adsorption behavior of MNZ onto CNC-RH, equilibrium adsorption data were analyzed using two common isotherm models: Langmuir and Freundlich.

The Langmuir isotherm assumes monolayer adsorption on a homogeneous surface and is expressed through a linear relationship, as shown in Equation (3) and illustrated in **Fig. 9**. In this model, Ce represents the equilibrium concentration of MNZ (mg/L), q_e is the amount of MNZ adsorbed per unit mass of CNC-RH (mg/g), and K_L (L/mg) is the Langmuir constant, which signifies the adsorption energy. The fundamental characteristics of the Langmuir isotherm can be assessed using the dimensionless separation factor K_L, where a value of 0.008 indicates that the adsorption is favorable. If K_L were equal to 0, the adsorption process would be irreversible.

The Freundlich isotherm (**Fig. 10**), in contrast, describes adsorption on a heterogeneous surface with multilayer adsorption. Its linear form is represented in Equation (5), where K_F denotes the maximum adsorption capacity (mg/g), and 1/n represents the adsorption intensity. Since n > 1, the adsorption of MNZ onto CNC-RH is confirmed to be a favorable physical process, as demonstrated in Equations (7) and (8).

By comparing the determination coefficient (R^2) values, it was observed that the Freundlich isotherm provided a better fit for the adsorption data than the Langmuir model (**Table 3**). This suggests that MNZ adsorption onto CNC-RH occurs on a heterogeneous surface with multilayer adsorption rather than a uniform monolayer. Furthermore, the n value greater than 1 reinforces the conclusion that the adsorption process is favorable.

Table 3. Isotherm models for the adsorption of metronidazole antibiotics using CNC-RH.

Models	Parameters	
Langmuir	q_m (mg/g)	0.044
	K_L (1/mg)	0.008
	R^2	0.999
Freundlich	K_F	-4.577
	n	38.42
	R^2	1

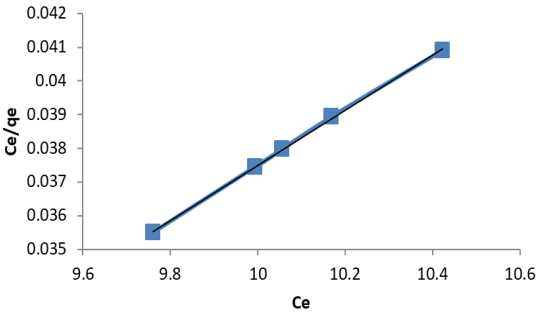

Fig. 9. Langmuir isotherm for the adsorption of metronidazole antibiotic using CNC-RH.

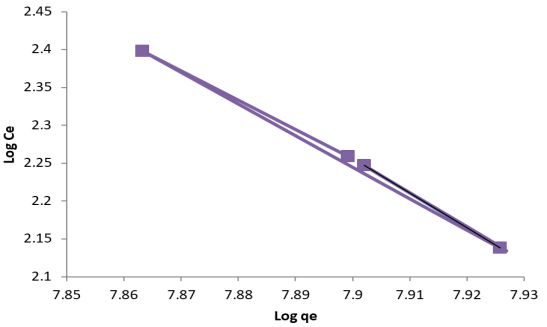

Fig. 10. Freundlich isotherm model for the adsorption of metronidazole antibiotic using CNC-RH.

Adsorption Kinetics of MNZ

Adsorption kinetics describe the rate at which MNZ is adsorbed onto CNC-RH, determining the equilibrium time. To assess the mass transfer rate of MNZ onto the adsorbent, kinetic models were applied using equilibrium test data, specifically the pseudo-first-order and pseudo-second-order models. The pseudo-first-order kinetic model assumes that adsorption occurs proportionally to the number of unoccupied adsorption sites and follows a linear form represented in Equation (3). In this model (**Fig. 11**), qt represents the adsorption capacity at time t, while k_1 is the pseudo-first-order rate constant. The pseudo-second-order kinetic model is based on solid-phase adsorption, assuming chemisorption as the rate-limiting step. The parameters qe (equilibrium adsorption capacity) and k_2 (pseudo-second-order rate constant) are obtained by plotting t/qe versus t, as expressed in Equation (4). Based on the kinetic constants and correlation coefficients (R^2) presented in **Table 4** and **Fig. 12**, along with the comparison between experimental and calculated data, it was observed that the adsorption kinetics followed the pseudo-second-order model. The model exhibited a perfect linearity ($R^2 \approx 1$), indicating that the adsorption of MNZ onto CNC-RH is primarily governed by chemisorption, involving valence forces or electron sharing between the adsorbent and adsorbate.

Table 4. Kinetic models for the adsorption of metronidazole antibiotic using CNC-RH.

Model	values
Pseudo first order	
q_e cal (mg/g)	4.820
K_1 (min^{-1})'	0.058
R^2	0.499
Pseudo second order	
qe cal (mg/g)	- 0.757
K_2 (g/mg min)	-2140
R^2	0.999

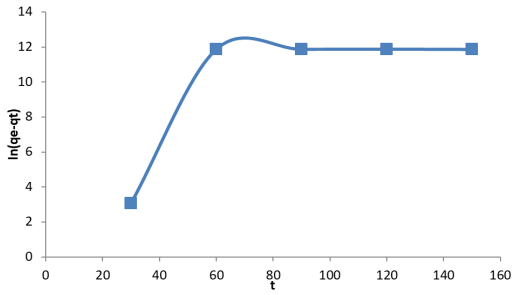

Fig. 11. Pseudo first order for the adsorption of metronidazole antibiotic using CNC-RH.

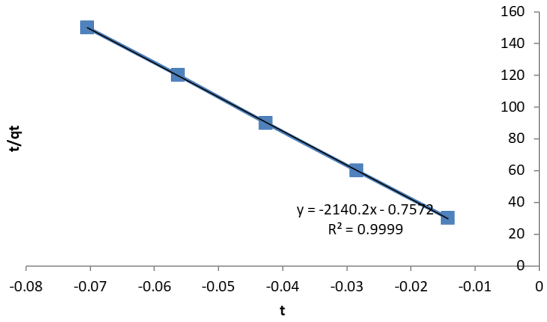

Fig. 12. Pseudo second order for the adsorption of metronidazole antibiotic using CNC-RH.

To investigate the reaction pathways and the potential rate-determining step in the adsorption of MNZ onto CNC-RH, two kinetic models—pseudo-first-order and pseudo-second-order—were applied. These models help determine how adsorption occurs, and which mechanism governs the process. The pseudo-first-order model assumes that the adsorption rate is proportional to the number of unoccupied adsorption sites. It is represented by a linear equation that allows for the determination of the rate constant (k_1) and adsorption capacity at a given time (q_t). The pseudo-second-order model considers that adsorption is controlled by chemical interactions (chemisorption) between the adsorbate and the adsorbent. This model involves the determination of the rate constant (k_2) and equilibrium adsorption capacity (q_e) by plotting t/q_e versus t. By comparing the correlation coefficients (R^2) and kinetic parameters obtained from both models, the adsorption process was best described by the pseudo-second-order model, indicating that chemisorption plays a dominant role in MNZ adsorption onto CNC-RH.

Thermodynamic Parameters for MNZ Removal

Thermodynamic parameters were evaluated to determine the feasibility and nature of the adsorption process. The parameters Gibbs free energy (ΔG), entropy (ΔS), and enthalpy (ΔH) were calculated at different temperatures (298 K, 303 K, 313 K, 323 K, and 333 K) using Equations (5), (6), and (7). The results are summarized in **Table 5**.

Table 5. Thermodynamic parameters for the adsorption of metronidazole antibiotics using CNC-RH.

Temperature (K)	ΔG(J/mol)	Δ***S***(J/molK)	ΔH(J/mol)
298	-103.566	0.482	40.07
303	-105.976		
313	-110.796		
323	-115.616		
333	-120.436		

The ΔG values ranged from -103.566 to -120.436 kJ/mol as the temperature increased from 298 K to 333 K. The negative ΔG values at all temperatures confirm that the adsorption of MNZ onto CNC-RH is spontaneous. Furthermore, the increasing magnitude of ΔG with temperature suggests that higher temperatures enhance the favorability of the adsorption process, consistent with previous findings [30]

The positive ΔH value indicates that the adsorption process is endothermic, meaning that energy is absorbed during adsorption. This suggests that increasing temperature facilitates the adsorption of MNZ onto CNC-RH. Additionally, the entropy change (ΔS) reflects increased randomness at the solid-liquid interface, further supporting the feasibility of the adsorption process.

CONCLUSION

This study effectively demonstrated the potential of rice husk-derived cellulose nanocrystals (CNC) as an efficient adsorbent for the removal of metronidazole (MNZ), a pharmaceutical contaminant. The CNC yield was 26.46%, and FTIR analysis verified the existence of functional groups that augment adsorption. The surface area and porosity of the material enhanced its adsorption efficiency. Crucial parameters, including MNZ concentration, adsorbent dosage, contact duration, pH, and temperature, were determined to substantially affect the adsorption process. Elevated MNZ concentrations and augmented adsorbent dosage resulted in enhanced removal efficiency, while an optimal temperature of 50°C was determined

to maximize adsorption. The process was determined to be spontaneous and endothermic, as evidenced by negative ΔG and positive ΔH values. Alkaline pH conditions and reduced contact durations were also advantageous. The adsorption behavior was optimally characterized by the Freundlich isotherm and pseudo-second-order kinetic models, indicating multilayer adsorption on heterogeneous surfaces and chemisorption processes. Rice husk-derived CNC offers a sustainable, cost-effective, and efficient solution for pharmaceutical wastewater treatment, supporting environmental remediation objectives and circular economy principles through the valorization of agricultural waste. Future research may investigate scalability and regenerative capacity to evaluate practicality in real-world applications.

REFERENCES

1. Allegre CM. Treatment and reuse of reactive dyeing effluents. J Memb Sci. 2006;269:15-7.
2. de Andrade JR, Oliveira MF, da Silva MGC, Vieira MGA. Adsorption of pharmaceuticals from water and wastewater using nonconventional low-cost materials: A review. Ind Eng Chem Res. 2018;57:3103–27.
3. Dolar D, Zokic TI, Kosutic K, Asperger D, Pavlovic DM. RO/NF membrane treatment of veterinary pharmaceutical wastewater: comparison of results obtained on a laboratory and a pilot scale. Environ Sci Pollut Res. 2012;19:1033–42.
4. Yenisoy-Karakas SA. Physical and chemical characteristics of polymer-based spherical activated carbon and its ability to adsorb organics. Carbon. 2004;42:477–84.
5. Adebowale KO, Kayode A. Mechanism on the sorption of heavy metals from binary solution by a low-cost montmorillonite and its desorption potential. Alexandria Eng J. 2015;54:757–67.
6. Rizakul A, Sadaf NS. Kinetics and thermodynamics studies of adsorption of methylene blue from aqueous solutions onto Paliurus spina-christi fruits and seeds. IOSR J Appl Chem. 2017;10(5):53–63.
7. Gupta A, Poddar PK, Jamari SS, Kim NS, Khan TA, Sharma S, et al. Synthesis of nanocellulose from rubberwood fibers via ultrasonication combined with enzymatic and chemical pretreatments. Asian J Appl Sci. 2015;3.
8. Isogai A, Wu CN, Saito T, Fujisawa S, Fukuzumi H. Ultrastrong and high gas-barrier nanocellulose/clay-layered composites. Biomacromolecules. 2012;13:1927–32.
9. Milanez DH, Amaral RM, Faria LIL, Gregolin JAR. Assessing nanocellulose developments using science and technology indicators. Mater Res. 2013;16:635–41.
10. Mahfoudhi N, Boufi S. Nanocellulose as a novel nanostructured adsorbent for environmental remediation: a review. Cellulose. 2017;1–27.
11. Suopajärvi T, Koivuranta E, Liimatainen H, Niinimäki J. Flocculation of municipal wastewaters with anionic nanocelluloses: influence of nanocellulose characteristics on floc morphology and strength. J Environ Chem Eng. 2014;2:2005–12.
12. Laitinen O, Kemppainen K, Ämmälä A, Sirviö JA, Liimatainen H, Niinimäki J. Use of chemically modified nanocelluloses in flotation of hematite and quartz. Ind Eng Chem Res. 2014;53:20092–8.
13. Barazzouk S, Daneault C. Amino acid and peptide immobilization on oxidized nanocellulose: spectroscopic characterization. Nanomaterials. 2012;2:187–205.
14. Shah J, Riaz M. Removal of Rhodamine B from aqueous solutions and wastewater by walnut shells: kinetics, equilibrium and thermodynamics studies. Front Chem Sci Eng. 2013;7(4):428–36.
15. Ali I, AL-Othman ZA, Alwarthan A. Synthesis of composite iron nano adsorbent and removal of ibuprofen drug residue from water. J Mol Liq. 2016;219:858–64.
16. Özer ET, Sarikaya AG, Osman B. Adsorption and removal of diethyl phthalate pharmaceuticals. Catal Today. 2016;241:47–54.
17. Boxall ABA, et al. Pharmaceuticals and personal care products in the environment: What are the big questions? Environ Health Perspect. 2012;120:1221–9.
18. Hammari AM, Abubakar AJ, Usman AB, Fatima MU, Judith S, Jauro BM. Synthesis and characterization of cellulose nano–crystals derived from groundnut shell for metronidazole antibiotic removal. Bima J Sci Technol. 2024;8(3B). doi:10.56892/bima.v8i3B.843
19. Ohwoavworhua FO, Okhamafe AO. Cellulose nanocrystals and nanofibrils obtained from corn straw by hydrolytic action of four acids: particulate, powder and tablet properties. Drug Discov Anal. 2020;14(34).
20. Marzo A, Dal Bo L. Chromatography as an analytical tool for selected antibiotic classes: a reappraisal addressed to pharmacokinetic application. J Chromatogr A. 1998;812(1-2):17–34.
21. Idan IJ, Abdullah LC, Choong TSY, Siti Nurul Ain B, Jamil MD. Equilibrium, kinetics and thermodynamic adsorption studies of acid dyes on adsorbent developed from kenaf core fiber. Adsorpt Sci Technol. 2017;1–19.
22. Hammari AM, Abubakar H, Misau MI, Aroke UO, Hamza UD. Adsorption equilibrium and kinetic studies of methylene blue dye using groundnut shell and sorghum husk biosorbent. J Environ Bioremediat Toxicol. 2020;3(2):32–9.
23. Kumar PS, Palaniyappan M, Priyadharshini M, Vigensh AM, Thonjiappan A, Sebastina PAF, et al. Adsorption of basic dye onto raw and surface-modified agricultural waste. Environ Prog Sustain Energy. 2013;33(1):87–98.
24. Hammari AM, Misau MI, Aroke UO, Hamza UD, Yusuf AA. Adsorption equilibrium and kinetics studies of Congo red dye using groundnut shell and sorghum husk biosorbent. J Biochem Microbiol Biotechnol. 2021;9(1):30–7.
25. Hammari AM, Hamza UD, Ibrahim M, Garba K, Muhammad IM. Innovative application of cellulose nano-crystals from agricultural waste for enhanced pharmaceutical wastewater treatment through artificial intelligence-driven adsorption modelling. Glob J Environ Sustain Stud. 2024. doi:10.69798/49168724
26. Kamaraj M, Umamaheswari P. Preparation and characterization of groundnut shell activated carbon as an efficient adsorbent for the removal of methylene blue dye from aqueous solution with microbiostatic activity. J Mater Environ Sci. 2017;8(6):2019–25.
27. Hassanzadeh M. Nanocellulose from the Appalachian hardwood forest and its potential applications [MSc Thesis]. West Virginia University; 2018. Available from: https://researchrepository.wvu.edu/etd/5780
28. Pourjavadi A, Mazaheri Tehrani Z, Jokar S. Chitosan-based supramolecular polypseudorotaxane as a pH-responsive polymer and their hybridization with mesoporous silica-coated magnetic graphene oxide for triggered anticancer drug delivery. Polymer. 2015;76:52–61.
29. Datugun P. Adsorption of dyes on sorghum husk and groundnut shell from agricultural wastes [MSc thesis]. Bauchi, Nigeria: Abubakar Tafawa Balewa University; 2018.
30. Enenebeaku KC, Okorocha JN, Akalezi OC. Adsorptive removal of methylene blue from aqueous solution using agricultural waste: equilibrium, kinetic and thermodynamic studies. Am J Chem Mater Sci. 2015;2(3):14–25.